Available online at www.sciencedirect.com
ScienceDirect
Nuclear Instruments and Methods in Physics Research B 259 (2007) 688–693
NIM B Beam Interactions with Materials & Atoms
www.elsevier.com/locate/nimb

The ^{40}Ca(α, γ)^{44}Ti reaction at DRAGON

C. Vockenhuber [a,*], C.O. Ouellet [b], L. Buchmann [a], J. Caggiano [a], A.A. Chen [b], J.M. D'Auria [c], D. Frekers [d], A. Hussein [e], D.A. Hutcheon [a], W. Kutschera [f], K. Jayamanna [a], D. Ottewell [a], M. Paul [g], J. Pearson [b], C. Ruiz [a], G. Ruprecht [a], M. Trinczek [a], A. Wallner [f]

[a] *TRIUMF, 4004 Wesbrook Mall, Vancouver, BC, Canada V6T 2A3*
[b] *McMaster University, Hamilton, ON, Canada*
[c] *Simon Fraser University, Burnaby, BC, Canada*
[d] *Institut für Kernphysik, Universität Münster, Germany*
[e] *University of Northern British Columbia, Prince George, BC, Canada*
[f] *Vienna Environmental Research Accelerator, Institut für Isotopenforschung und Kernphysik, Universität Wien, A-1090 Wien, Austria*
[g] *Racah Institute of Physics, Hebrew University, Jerusalem, Israel*

Available online 4 Februray 2007

Abstract

Nuclear reactions play a key role in understanding nucleosynthesis in stars. Recoil mass spectrometers such as DRAGON are well suited to study reactions with respect to astrophysical production because of direct detection of reaction products. Here we present the first stage of an experiment running at the recoil mass spectrometer DRAGON at the ISAC/TRIUMF facility in Vancouver, Canada, to study the reaction ^{40}Ca(α, γ)^{44}Ti at astrophysically relevant energies. This reaction is one of the key reactions for production of ^{44}Ti, which has been identified in young supernova remnants by space based γ-ray telescopes onboard COMPTEL and INTEGRAL. In this paper we focus on technical upgrade of DRAGON for ^{40}Ca(α, γ)^{44}Ti and preliminary results at resonances at $E_x \sim 9.2$ MeV.

PACS: 25.40.Lw; 26.30.+k; 29.30.Aj

Keywords: ^{44}Ti; Recoil mass spectrometer; Radiative capture

1. Introduction

^{44}Ti ($t_{1/2} = 58.9 \pm 0.3$ yr [1]) is an interesting nuclide for astrophysics. The detection of ^{44}Ti through the 1.157 MeV γ-ray line by COMPTEL in supernova remnant Cas A [2] has generated a great interest in ^{44}Ti. The light curves from the ^{44}Ti decay of relatively recent and nearby supernovae provide an observational test for nucleosynthesis models. Today, the measurement of ^{44}Ti from known and as yet unknown supernovae has high priority in the current γ-ray astronomy mission of INTEGRAL [3–5]. In addition to the observation in space, excess of ^{44}Ca found in presolar grains indicates significant ^{44}Ti production in supernovae [6].

^{44}Ti is produced primarily in the α-rich freeze-out from nuclear statistical equilibrium, which takes place in the last stage of a supernova when at low densities α-particles are available for capture reactions on heavier nuclei. The calculation of the ejected amount of ^{44}Ti in a core-collapse supernova depends on the mass cut, the pre-supernova composition and the maximum temperature and density reached in the ejecta. All of them are still very uncertain. Also the nuclear reaction rates related to ^{44}Ti production are still uncertain. However, a clear picture of ^{44}Ti nucleosynthesis will improve our understanding of supernovae.

* Corresponding author.
E-mail address: christof.vockenhuber@triumf.ca (C. Vockenhuber).

0168-583X/$ - see front matter © 2007 Elsevier B.V. All rights reserved.
doi:10.1016/j.nimb.2007.01.222

Nuclear reactions governing the nucleosynthesis of ^{44}Ti were studied in detail by [7]. They give a dependence of the final ^{44}Ti yield on various nuclear reactions in order of significance under different astrophysical conditions. Since the reaction ^{40}Ca(α, γ)^{44}Ti is the main process for the nucleosynthesis of ^{44}Ti, it has a strong influence on the final ^{44}Ti yield.

This reaction was studied in the past by prompt γ-ray spectrometry in the energy range of $E_\alpha = 3.5$–4.6 MeV [8] and $E_\alpha = 2.75$–4.00 MeV [9], which correspond to stellar temperatures of $T_9 = 1.7$–2.2 and $T_9 = 1.2$–2.1, respectively ($T_9 = T/10^9$ K). Resonance strengths were measured for 12 isolated narrow resonances. At higher energies ($E_\alpha = 4.5$–6 MeV) the resonance strengths of other states were measured by [10], including the rather strong resonance at $E_\alpha = 4.52$ MeV, which was later identified as an isospin-mixed triplet at energy levels of ^{44}Ti $E_x = 9.215$, 9.227 and 9.239 MeV [11].

A recent off-line measurement using Accelerator Mass Spectrometry (AMS) for counting of ^{44}Ti atoms from a preceding ^{40}Ca irradiation of a He gas target confirmed the yield at $E_x \sim 9.2$ MeV [12], but showed a significantly larger production rate at wider temperature region $T_9 \sim 0.8$–3 [13,14] compared to the expected yield from prompt γ-ray spectrometry.

In order to get a better understanding of ^{44}Ti nucleosynthesis we are pursuing a detailed study of the reaction ^{40}Ca(α, γ)^{44}Ti in inverse kinematics at astrophysically relevant energies with the recoil mass spectrometer Detector for Recoils And Gamma rays Of Nuclear reactions (DRAGON) located at the ISAC facility at TRIUMF in Vancouver, Canada. Here we describe the experimental apparatus as well as first results at the strong resonances at $E_x \sim 9.2$ MeV.

It is interesting to note the similarities in the experimental challenges between AMS and the present detection of an on-line produced nuclide: isobaric purity of the incident beam, physical separation and discrimination of the rare nuclide from the main beam.

2. Ion source and beam contamination

The experiment requires a ^{40}Ca beam in the energy range of 0.5–1.2 MeV/u. ^{40}Ca beam is produced in the off-line ion source OLIS. Because of the restrictions of ISAC's RFQ ($A/q < 30$) a charge state of 2+ or higher must be extracted by the ion source. Beam contamination is another concern since ^{40}Ar is a stable isobar of ^{40}Ca (^{40}K is negligible due to its low isotopic abundance of 0.0117%). ^{40}Ar is the most abundant isotope of Ar and common in gas ion sources. The ^{40}Ar contamination is not critical for ^{44}Ti production, but high intensities of ^{40}Ar can cause problems with stripper foil lifetimes and beam normalization, especially if the ^{40}Ca/^{40}Ar ratio is not constant. Another potential contamination to ^{40}Ca^{2+} is ^{20}Ne^{+}.

Our first approach was using the surface-hybrid ion source, loaded with pure Calcium. Ca has a first ionization potential of 6.1 eV and can be easily ionized by surface ionization. Due to the high first ionization potentials of Ar (15.8 eV) and Ne (21.6 eV) these elements are not ionized at significant levels in a surface ion source. The second ionization potential of all elements is above 10 eV and thus multiple charge states are usually not observed with surface ion sources. However, the special design of the OLIS hybrid-surface ion source allows electron impact ionization as a second ionization step. This results in a significant production of 2+ charge states of ^{40}Ca. Furthermore, the significant electron current of about 100 μA screens and carries the 2+ ions through the retarding potential at the extraction electrode. This technique provides a clean ^{40}Ca^{2+} beam up to a few nA with negligible contamination of ^{40}Ar and other components (Fig. 1(a)).

In order to achieve higher beam currents a micro-wave ion source was used. Clean He gas was used for the plasma which sputters Ca atoms from a large pure Ca metal target installed at the back of the ion source chamber. Up to several 100 nA could be produced with little contamination of ^{40}Ar (Fig. 1(b)). The large sputtering target allows an operation of several weeks without interruptions. Most of the results in this paper were performed with a ^{40}Ca beam from the micro-wave ion source because of the higher beam current.

The ^{40}Ca^{2+} beam was then accelerated through a room-temperature radio-frequency quadrupole (RFQ) to 153 keV/u where it was stripped to higher charge states

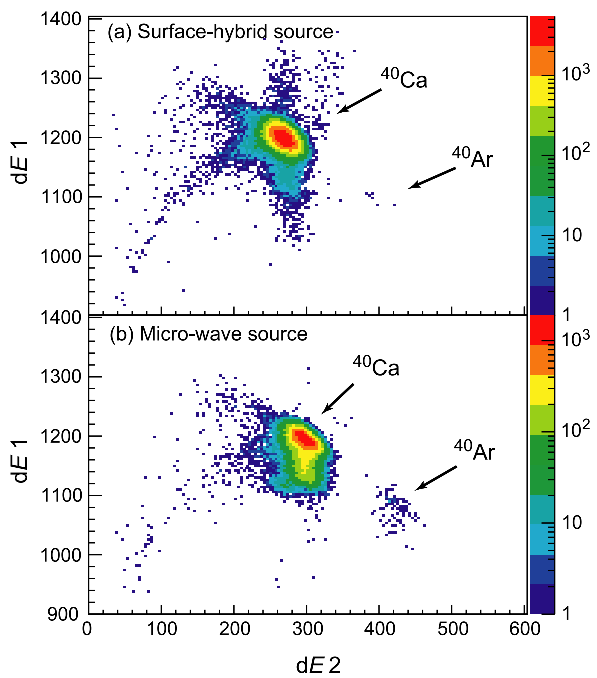

Fig. 1. Beam contamination from the ion sources. A ^{40}Ar/^{40}Ca ratio of 8×10^{-5} for the surface-hybrid source (a) and 5×10^{-3} for the micro-wave source (b) was measured using attenuated beam in the DRAGON ionization chamber (dE1 and dE2 are the two energy-loss signals from the segmented anode of the ion chamber, see Section 3.4). Spectra were taken at rather high count rates (10^3–10^4 cts/s). At this rate pile-up and peak distortions are visible.

using a thin carbon foil. Charge state 7+ was selected for further acceleration through a drift tube linac (DTL) to the final beam energy of 1.135 MeV/u. An overview of the ISAC accelerators can be found in [15].

3. Recoil mass separator DRAGON

In the following section the recoil mass separator DRAGON is described briefly with focus on modifications for the $^{40}Ca(\alpha,\gamma)^{44}Ti$ reaction. Details about construction and commissioning of DRAGON can be found in [16,17].

3.1. Gas target and BGO γ-ray detector array

The beam hits the DRAGON windowless gas target which is filled with ^4He gas up to 8 Torr, corresponding to 3×10^{18} ^4He atoms/cm^2, to ensure the energy loss (∼100 keV/Torr) is larger than the energy width of the resonances. The gas target is surrounded by a γ-ray detector array consisting of 30 tightly packed BGO crystals connected to photomultipliers which cover 90% of 4π solid angle as viewed from the center of the 12.3 cm long gas target. Prompt γ-rays from the reaction are identified using coincidence with the detected recoil ^{44}Ti at the DRAGON end detector. The efficiency of the BGO array depends on the γ energy as well as on the γ-ray multiplicity. The single γ-ray efficiency is between 40% and 60% for γ-ray energies of 1–10 MeV.

3.2. Electromagnetic mass separator

The sparse recoils are separated from incoming beam by the electromagnetic mass separator. It comprises two stages, each with a magnetic and an electrostatic dipole providing an achromatic focus after each section at the mass and final slits respectively. Since in capture reactions beam and recoils have the same momentum, the main separation comes from the electrostatic dipoles. The reason for the first element being magnetic is to first provide a charge selection without having non-selected ions hitting electrodes under glancing angles [16].

The ion optics of the separator is designed to transport recoils with a cone angle of ±20 mrad and ±5% energy spread. A series of quadrupoles focuses the beam and four sextupoles correct for higher order abberations. For this particular reaction the recoil cone angle due to the kick from the γ-ray is maximal ±5 mrad and thus well within the design of the spectrometer.

The total suppression of beam in the separator depends on various factors like beam quality, target thickness, ion energy, ion mass and slit openings. Suppression factors for proton capture reaction range from 10^{13} at high energies (∼1.25 MeV/u) down to 10^8 at low energies (∼0.2 MeV/u).

In α-capture reactions beam which still reaches the end detector (leaky beam) usually has lower energy and depends strongly on the analyzed charge state. This is different from proton capture reactions where leaky beam tends to have the full beam energy. The reason is that the next lower charge state of ^{40}Ca is closer in A/q to ^{44}Ti and thus ions with lower energy can easier leak through the separator. The suppression factor of the separator S depends strongly on the selected ^{44}Ti charge state (see Fig. 2) and is calculated from the number of ^{40}Ca on target N_{target} and the number of leaky ^{40}Ca detected N_{detector} corrected for the charge state fraction F_{q} (see Section 3.3):

$$S(q) = \frac{N_{\mathrm{target}}}{N_{\mathrm{detector}}} F_{\mathrm{q}}. \qquad (1)$$

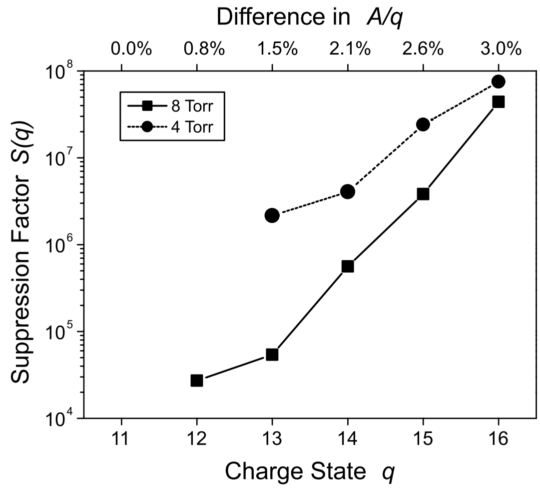

Fig. 2. ^{40}Ca suppression factor of the spectrometer (without γ coincidence and cuts on IC signals) depending on selected ^{44}Ti charge state. The two different He target pressures were measured at different runs and beam quality may have changed as well. The difference in A/q shown on the top axis is defined as $(44/q - 40/(q-1))/(44/q)$.

The worst case is ^{44}Ti in charge state 11+ where $^{40}Ca^{10+}$ has exactly the same A/q and thus there is no chance for separation if ^{40}Ca ions loose a little energy so that they have the same E/q as ^{44}Ti. To this end the suppression is much lower in α-capture reaction of heavy ions and depends on the selected charge state. The suppression factor was improved during a later stage of the experiment due to better beam tune.

3.3. Charge state booster

One limitation of the DRAGON recoil separator is the bending requirement of the electrostatic and magnetic dipoles. During this experiment we were limited to voltages up to ±175 kV for the first electrostatic dipole ED1. This had serious implications of the useable charge states. Only charge states 13+ or higher for 1.13 MeV/u ^{40}Ca beam and 12+ or higher for ^{44}Ti recoils could be used. However, the mean charge state after the gas is 11.0 (for ^{40}Ca), too far away from dipole specifications.

Therefore we developed the DRAGON charge state booster (CSB). It consists of a foil which can be placed right after the window less gas target. The basic idea is that solid stripping media result in higher charge states of passing ions. One challenge was the gas jet coming out of inner gas target box which destroyed any C-foil (20 μg/cm^2) immediately. Thus we used more robust silicon nitride windows of 50 nm and 100 nm thickness (=17 and 34 μg/cm^2, respectively) from Silson Ltd., Northampton, UK. We could use gas pressures up to 8.5 Torr without damaging the foil. To avoid any further stripping after the CSB foil it has to seal the downstream beam line efficiently from the gas flow out of the gas target box. The foil has to be retractable in order not to disturb the beam tuning procedure through the gas target. This was accomplished using a specially designed sliding mechanism which is driven by a model air plane servo. The life-time of a 100 nm SiN foil under ~1.1 MeV/u ^{40}Ca beam irradiation is up to 600 pnA h, much longer than the carbon foils used for stripping between the accelerators.

We measured charge state distributions for ^{40}Ca and ^{40}Ar by measuring current in a Faraday cup after the first bending magnet MD1 (Fig. 3). Charge state fractions F_q were calculated by normalizing to the current in a Faraday cup upstream of the gas target. Charge states 11+ or higher can be bent with MD1. As shown by [18] a Gaussian can be fitted to the data points to get the full charge state distribution. The final CSB setup shifted the charge state distribution as expected (according to the semi-empirical formula of Sayer [19]) without and with gas in the gas target (Fig. 3).

The CSB has several advantages: First, we can cover at least 2/3 of the charge state distribution of ^{44}Ti recoils. Second, we can avoid the unfavorable charge states 10+ and 11+, where the beam suppression of the recoil separator is reduced due to identical A/q values of beam and recoil. Third, for a given energy the recoils leave the CSB with the same charge state fraction no matter where the reaction occurs. Otherwise, with only the gas acting as a stripper, the charge state fraction depends strongly on the position where the reaction takes place because the equilibrium distribution is not reached at our pressures. This is particularly important if a thick target (high He gas pressure) is used where resonances can occur at various locations along the beam path in the gas.

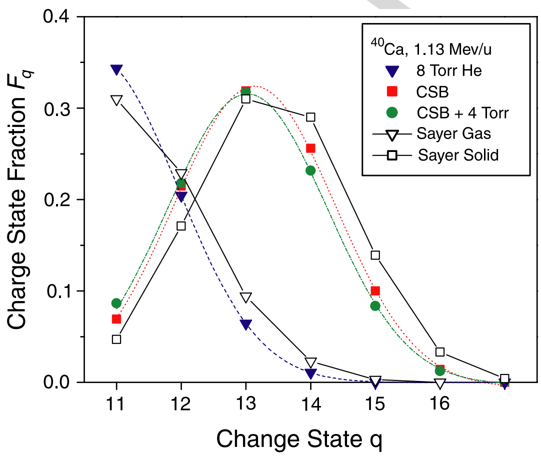

Fig. 3. Measured charge state distributions of ^{40}Ca at 1.13 MeV/u with and without He gas and charge state booster (CSB). A Gaussian was fitted to the measured data points. For comparison the expected values from the Sayer formula for gas and solid medium are also shown as open symbols.

3.4. ^{44}Ti identification with an ionization chamber

Recoils are finally detected in the DRAGON ion chamber. It consists of an isobutane gas volume of 25 cm length separated from the upstream beam line by a thin entrance window (130 μg/cm^2 Mylar or grid supported 55 μg/cm^2 poly-propylene) of 50 mm diameter. In its volume ions lose energy according to their stopping power dE/dx, which depends on energy E, mass A and nuclear charge Z of the ions. The ionization products along the path of the ions are collected by a moderate electric field (50 V/cm) and lead to measurable signals at the anode, which is segmented into two 10 cm sections and a 5 cm section at the end of the chamber (dE1 for the first segment and dE2 for the second segment). A Frisch grid electrically separates the anode from the collecting volume. The gas pressure is adjusted to stop the ions before the end of the second segment. The total energy is measured as the sum of all segments with a resolution of 1.2% FWHM.

Because of the nature of leaky beam a single energy measurement is not enough for a clear identification of ^{44}Ti. Fig. 4 shows two-dimensional spectra (dE1 versus

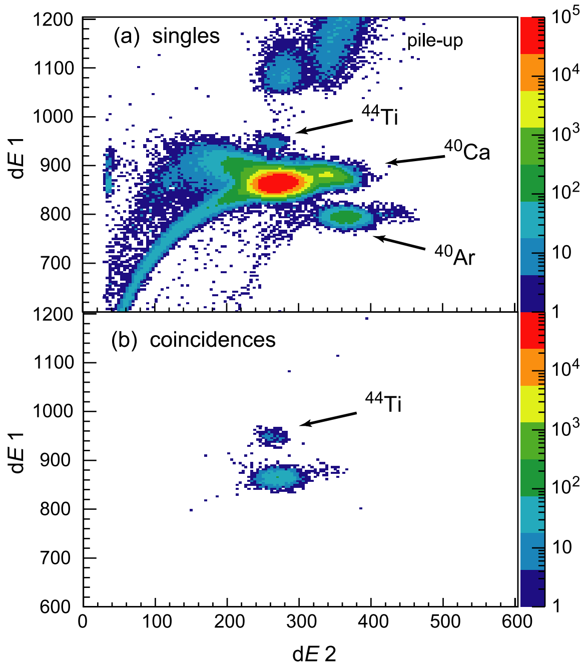

Fig. 4. Two-dimensional spectra (dE1 versus dE2) of singles (a) and coincidences with the BGO detector (b) of a typical run at the strong resonances. The main peak in singles is leaky ^{40}Ca, which is reduced in the coincidence spectrum by more than 3 orders of magnitude. The reduction of the ^{44}Ti counts from 402 (singles) to 251 (coincidences) is only due to the efficiency of the BGO detector. A small contamination of ^{40}Ar is visible.

dE2) of singles and coincidences with the BGO detector of a typical run at the strong resonances. ^{44}Ti signals are clearly separated from the broad background of leaky ^{40}Ca.

The ion chamber provides also identification of beam contamination (Fig. 1). Although ^{40}Ca and ^{40}Ar have the same energy they are clearly separated in the dE1 versus dE2 plot due to the difference in nuclear charge of 2.

4. ^{44}Ti yield at $E_x \sim 9.2$ MeV

In order to check the measurement capabilities of this reaction at DRAGON we started with the strong and well established resonances at $E_x \sim 9.2$ MeV. Resonance strengths and γ-ray decays of this isospin-mixed triplet were measured in detail by prompt γ-ray spectrometry [11].

The measurement of the resonance strength $\omega\gamma$ is based on the thick target yield, Y, which is the number of recoils per incoming projectile

$$Y = \frac{\lambda^2}{2} \frac{m_p + m_t}{m_t} \left(\frac{dE}{dx}\right)^{-1} \omega\gamma \qquad (2)$$

with λ the de Broglie wavelength of the reduced mass of the compound system, m_p and m_t the mass of projectile and target, dE/dx the stopping power of the projectile in the target in the laboratory system and $\omega\gamma$ defined as:

$$\omega\gamma = \frac{2J_R + 1}{(2J_t + 1)(2J_p + 1)} \frac{\Gamma_\alpha \Gamma_\gamma}{\Gamma} \qquad (3)$$

with J_R, J_t and J_p the spins of the resonance, target and ground state of projectile, respectively and Γ_α, Γ_γ the partial α and γ widths of the resonance and $\Gamma = \Gamma_\alpha + \Gamma_\gamma$.

The yield of ^{44}Ti was measured at several ion energies and target pressures to resolve the narrow structure at $E_x \sim 9.2$ MeV. Due to the high yield, charge states 12+ to 16+ of ^{44}Ti could be measured. This allowed us to measure the charge state distribution of ^{44}Ti recoils and derive the absolute yield.

The beam normalization is based on elastic monitors which consists of a Si detector measuring elastically scattered He atoms under a well defined angle of 57°. Assuming pure Rutherford scattering, a correlation factor independent of beam energy and target pressure between beam current and elastically scattered He atoms is given by:

$$R = \frac{I}{eq} \frac{\Delta t P}{N_{He} E_b^2} \qquad (4)$$

with N_{He} the number of elastically scattered He atoms within Δt, I the beam current in front of the gas target in charge state q, E_b the beam energy in keV/u, P the He gas pressure in Torr and e the elemental charge. A variety of runs under different conditions were used to define $R = 1649 \pm 60$ Torr/(keV/u)^2. The error is dominated by the scatter of different runs. The incident beam intensity is then calculated using

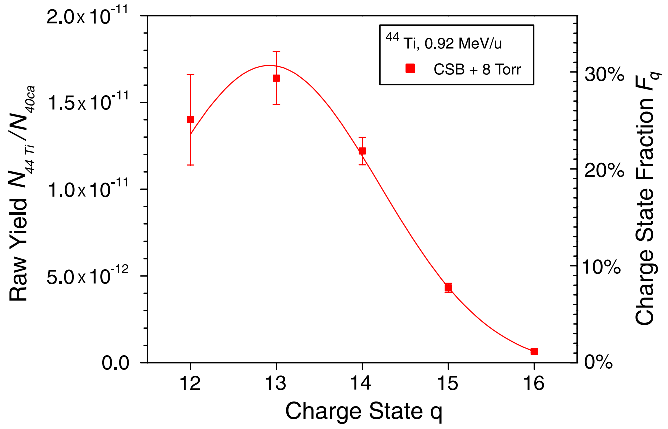

Fig. 5. Raw yield of coincidence ^{44}Ti recoils measured at 8 Torr He gas pressure. At this beam energy (1.135 MeV/u) and target thickness all three resonances at $E_x \sim 9.2$ MeV contribute to the yield. Error bars represent statistical uncertainties only.

$$N_{^{40}Ca} = \frac{N_{He} R E_b^2}{P}. \qquad (5)$$

The measured yield is calculated from:

$$Y = \frac{N_{^{44}Ti}}{N_{^{40}Ca} F_q \epsilon}, \qquad (6)$$

with F_q the charge state fraction of the recoils and ϵ the detection efficiency of the ^{44}Ti recoils which includes the transmission through the spectrometer and the efficiency of the end detector, both close to 100%. If coincidence with the γ-rays is used then ϵ includes the efficiency of the BGO detector array. In our case, where we have a clear recoil peak in the singles spectrum, $\epsilon = 0.624 \pm 0.039$ is determined from the ratio of ^{44}Ti counts between the singles and coincidence spectrum (see Fig. 4). If only the coincidence spectrum gives a clear recoil peak, GEANT simulations are used to estimate the BGO efficiency [20].

The charge state distribution F_q of ^{44}Ti recoils is calculated from the raw yield divided by the area of a Gaussian fit to the raw yield data (Fig. 5).

Using Eq. 6 we get a preliminary value for the ^{44}Ti yield for the sum of the isospin triplet at $E_x \sim 9.2$ MeV of $Y = 8.96 \pm 0.79 \times 10^{-11}$. This corresponds to a sum resonance strength of $\sum \omega\gamma = 7.7 \pm 0.7$ eV using the stopping power dE/dx = 39.4 keV/(μg/cm^2) from SRIM [21]. The uncertainty in our value consists of 5% beam normalization, 3.5% recoil counting statistics and 6.4% BGO efficiency. Not included are uncertainties from charge state distribution of ^{44}Ti recoils, which will be measured more precisely with stable Ti beam of the same velocity.

5. Summary and outlook

We have demonstrated the capability to measure ^{44}Ti recoils directly from the reaction ^{40}Ca(α,γ)^{44}Ti using the DRAGON recoil mass spectrometer. Our result at $E_x \sim 9.2$ MeV agrees with the measurements from prompt

γ spectroscopy (sum of resonance strengths $\sum \omega\gamma = 8.3 \pm 0.4$ eV measured by [11]) and off-line AMS (7.4 ± 2.5 eV [12]).

Measurements at the astrophysically interesting region from $E_x = 9.2$ MeV down to $E_x \sim 6.5$ MeV are in progress. The excitation function is measured using a thick target (up to 8 Torr He). The energy loss of ^{40}Ca in He gas is about 2.5 keV/u/Torr; thus we can scan the energy range $E_{\mathrm{lab}} = 1.13$ MeV/u down to $E_{\mathrm{lab}} \sim 0.5$ MeV/u with 30 steps at 8 Torr. Since the recoil spectrometer is in first order achromatic, small energy variations are focused to the same point at the end detector. The energy acceptance of the recoil spectrometer (about $\pm 5\%$) is sufficient to accept the energy range covered by the energy loss of ^{40}Ca at the He target. Energy-loss straggling in the CSB foil is about 0.5% and much smaller than the energy loss in the gas. In order to resolve interesting regions lower gas target pressures ($\sim$1 Torr) will be used.

Acknowledgements

We gratefully thank Marco Marchetto and Bob Laxdal for delivering ^{40}Ca beam to DRAGON and Peter Machule and Don Dale for assistance especially in connection with our first electrostatic dipole. We also acknowledge the help from our summer students Heather Crawford, Benji Wales and Lisa Fogarty during the measurement runs.

References

[1] I. Ahmad, J.P. Greene, E.F. Moore, S. Ghelberg, A. Ofan, M. Paul, W. Kutschera, Improved measurement of the ^{44}Ti half-life from a 14-year long study, Phys. Rev. C 74 (2006) 065803.

[2] A.F. Iyudin, R. Diehl, H. Bloemen, W. Hermsen, G.G. Lichti, D. Morris, J. Ryan, V. Schoenfelder, H. Steinle, M. Varendorff, C. de Vries, C. Winkler, COMPTEL observations of Ti-44 gamma-ray line emission from CAS A, Astron. Astrophys. 284 (1994) L1.

[3] F. Lebrun, B. Cordier, A. Iyudin, ^{44}Ti lines in the INTEGRAL core programme data, in: ESA SP-459 Exploring the Gamma-Ray Universe, 2001, p. 509.

[4] M. Renaud, F. Lebrun, R. Terrier, N. Prantzos, A. Decourchelle, J. Ballet, The study of young galactic supernovae through ^{44}Ti gamma-ray line emission with Integral, 35th COSPAR Scientific Assembly, 2004, p. 2694.

[5] R. Diehl, N. Prantzos, P. von Ballmoos, Astrophysical constraints from gamma ray spectroscopy, Nucl. Phys. A 777 (2006) 70.

[6] L.R. Nittler, S. Amari, E. Zinner, S.E. Woosley, R.S. Lewis, Extinct ^{44}Ti in presolar graphite and sic: proof of a supernova origin, Astrophys. J. 462 (1996) L31.

[7] L.-S. The, D.D. Clayton, L. Jin, M.S. Meyer, Nuclear reactions governing the nucleosynthesis of ^{44}Ti, Astrophy. J. 504 (1998) 500.

[8] J.J. Simpson, W.R. Dixon, R.S. Storey, Study of ^{44}Ti by the ^{40}Ca(α,γ)^{44}Ti reaction, Phys. Rev. C 4 (1971) 443.

[9] E.L. Cooperman, M.H. Shapiro, H. Winkler, Helium burning of ^{40}Ca, Nucl. Phys. A 284 (1977) 163.

[10] W.R. Dixon, R.S. Storey, J.J. Simpson, Levels of ^{44}Ti from the ^{40}Ca(α,γ)^{44}Ti reaction, Phys. Rev. C 15 (1977) 1896.

[11] W.R. Dixon, R.S. Storey, J.J. Simpson, An isospin-mixed triplet in ^{44}Ti, Can. J. Phys. 58 (1980) 1360.

[12] M. Paul, C. Feldstein, I. Ahmad, D. Berkovits, C. Bordeanu, J. Caggiano, S. Gehlberg, J. Goerres, J. Greene, M. Hass, A. Heinz, D. Henderson, S.K. Hiu, R.V.F. Janssens, C.L. Jiang, S. Jiang, Y. Nirel, R.C. Pardo, T. Pennington, K.E. Rehm, G. Savard, G. Verri, R. Vondrasek, I. Wiedenhover, M. Wiescher, Counting ^{44}Ti nuclei from the ^{40}Ca(α,γ)^{44}Ti reaction, Nucl. Phys. A 718 (2003) 239c.

[13] H. Nassar, M. Paul, S. Ghelberg, A. Ofan, N. Trubnikov, Y. Ben-Dov, M. Hass, B.S.N. Singh, Study of the supernova nucleosynthesis ^{40}Ca(α,γ)^{44}Ti reaction: progress report, Nucl. Phys. A 758 (2005) 411.

[14] H. Nassar, M. Paul, I. Ahmad, Y. Ben-Dov, J. Caggiano, S. Ghelberg, S. Goriely, J.P. Greene, M. Hass, A. Heger, A. Heinz, D.J. Henderson, R.V. Janssens, C.L. Jiang, Y. Kashiv, B.S. Nara Singh, A. Ofan, R.C. Pardo, T. Pennington, K.E. Rehm, G. Savard, R. Scott, R. Vondrasek, ^{40}Ca(α,γ)^{44}Ti reaction in the energy regime of supernova nucleosynthesis, Phys. Rev. Lett. 96 (2006) 041102.

[15] R.E. Laxdal, ISAC at TRIUMF: Status of the post-accelerator, in: International Workshop on Production of Radioactive Ion Beams (PRORIB 2001), Pui, India, 200, URL: www.triumf.ca/download/lax/prorib2000/prorib2001paper/prorib2000_3.pdf.

[16] D.A. Hutcheon, S. Bishop, L. Buchmann, M.L. Chatterjee, A.A. Chen, J.M. D'Auria, S. Engel, D. Gigliotti, U. Greife, D. Hunter, A. Hussein, C. Jewett, N. Khan, A. Lamey, W. Liu, A. Olin, D. Ottewell, J.G. Rogers, G. Roy, H. Sprenger, C. Wrede, The DRAGON facility for nuclear astrophysics at TRIUMF-ISAC, Nucl. Instr. and Meth. A 498 (2003) 190.

[17] S. Engel, D.A. Hutcheon, S. Bishop, L. Buchmann, J. Caggiano, M.L. Chatterjee, A.A. Chen, J.M. D'Auria, D. Gigliotti, U. Greife, D. Hunter, A. Hussein, C. Jewett, A. Laird, A. Lamey, W. Liu, A. Olin, D. Ottewell, J. Pearson, C. Ruiz, G. Ruprecht, M. Trinczek, C. Vockenhuber, C. Wrede, Commissioning the DRAGON facility at ISAC, Nucl. Instr. and Meth. A 553 (2005) 491.

[18] W. Liu, G. Imbriani, L. Buchmann, A.A. Chen, J.M. D'Auria, A. D'Onofrio, S. Engel, L. Gialanella, U. Greife, D. Hunter, A. Hussein, D.A. Hutcheon, A. Olin, D. Ottewell, D. Rogalla, J. Rogers, M. Romano, G. Roy, F. Terrasi, Charge state studies of low energy heavy ions passing through hydrogen and helium gas, Nucl. Instr. and Meth. A 496 (2003) 198.

[19] R.O. Sayer, Semi-empirical formulars for heavy-ion stripping data, Rev. de Phys. Appl. 12 (1977) 1543.

[20] D. Gigliotti, Efficiency calibration measurement and geant simulation of the dragon bgo gamma ray array at triumf, Ph.d. thesis, Univ. of Northern British Columbia, 2004.

[21] J.F. Ziegler, J.P. Biersack, U. Littmark, The Stopping and Range of Ions in Solids, Pergamon Press, New York, 1985.